Characterization of Micro- and Mesoporosity in SBA-15 Materials from Adsorption Data by the NLDFT Method

Peter I. Ravikovitch and Alexander V. Neimark*

Center for Modeling and Characterization of Nanoporous Materials, TRI/Princeton, 601 Prospect Ave, Princeton, New Jersey 08542-0625

Received: February 16, 2001; In Final Form: May 3, 2001

SBA-15 siliceous materials templated using triblock copolymers have recently received considerable attention because of their potential applications in catalysis and separations of large molecules. SBA-15 materials possess a regular hexagonal array of cylindrical channels of 5−30 nm in diameter and, unless specially treated, an appreciable volume of intrawall pores which may constitute up to 30% of the total porosity. The intrawall pores include micropores within the silica matrix and also mesopores that are narrower than the main channels. We present a consistent method for evaluating the pore structure parameters of SBA-15 materials from the nitrogen adsorption isotherms. The proposed method is based on the nonlocal density functional theory (NLDFT) of adsorption and capillary condensation in cylindrical pores. The NLDFT method allows one to calculate the mesopore size distribution and to evaluate the pore wall thickness and the amount of intrawall porosity. The structural parameters obtained by the NLDFT method are in agreement with geometrical considerations and X-ray diffraction data. Interpretation of adsorption isotherms on SBA-15 by means of the NLDFT method resolves some of the recently published discrepancies between the pore sizes determined from different methods. The NLDFT method is applicable to other micro−mesoporous materials.

1. Introduction

Siliceous mesoporous materials SBA-15, prepared by block copolymer templating, possess a regular two-dimensional array of tubular channels.[1,2] These materials have recently attracted considerable attention because of their promising applications in shape-selective catalysis, separations involving large molecules, etc.[3−23] In comparison with other regular mesoporous materials, e.g., MCM-41,[24] SBA-15 can be prepared with larger pores, up to 30 nm, resulting in a more stable structure because of thicker pore walls.[1,2] SBA-15 materials discussed in this work[1,4,17,18,21] were synthesized by using triblock copolymers of $EO_m-PO_n-EO_m$ type as structure directing agents; here, EO and PO stand for poly(ethylene oxide) and poly(propylene oxide), respectively. The structure of pore walls in the resulting organic−inorganic composite is best described as a mutual interpenetrating network of silica and poly(ethylene oxide) chains as supported by the NMR data.[25,26] Removal of the polymer leads to the development of irregular *intrawall* pores. Thus, SBA-15 materials generally possess rough pore walls with micro- and narrow mesopores that coexist with the regular hexagonal framework of main channels, as has been shown by Kruk et al.[17] Recent works of Ryoo and co-workers on the preparation of platinum[18] and carbon[19] replicas of SBA-15 demonstrate that the intrawall micropores form a continuous network that connects adjacent main channels. The structural parameters of SBA-15 depend significantly on the synthesis temperature, the procedure for the surfactant removal,[17] and the heat treatment.[18] In our discussion, we hypothesize that the pore structure of SBA-15 can be described in terms of the main channels and intrawall pores. The latter may include both micropores within the silica matrix as well as surface pores because of the roughness of the main channels as shown schematically in Figure 1. At this stage, we do not attempt a detailed characterization of the intrawall porosity. Our goal is to determine the size distribution of the main channels and the total amount of the intrawall porosity.

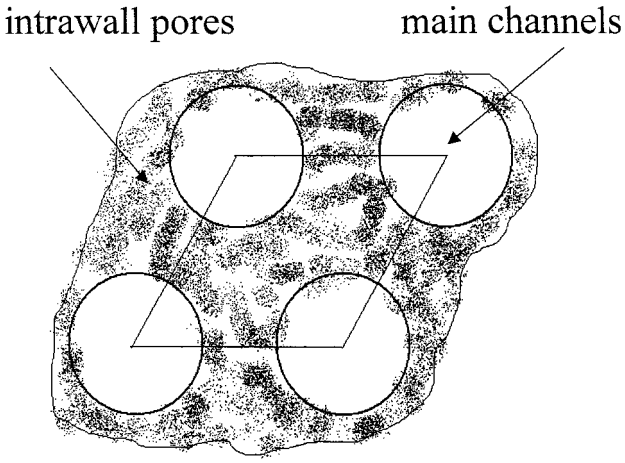

Figure 1. Schematic representation of SBA-15 structure.

Low temperature nitrogen adsorption isotherms are commonly used to evaluate the pore structure parameters of mesoporous materials, particularly SBA-15.[4−7,11−13,17,20,21] However, determination of the pore structure parameters of SBA-15 materials is complicated by two major factors: (1) the presence of intrawall porosity and (2) adsorption−desorption hysteresis. Usually, the micropore volume in micro−mesoporous materials can be determined from the comparison plot or similar (t-plot and alpha-S plot) methods,[27] which were applied in several studies of SBA-15 materials.[4,18,20,21] As will be shown below, the comparison plot method underestimates the total amount

* To whom correspondence should be addressed. E-mail: ravikovi@triprinceton.org; aneimark@triprinceton.org.

10.1021/jp010621u CCC: $20.00
Published on Web 06/20/2001

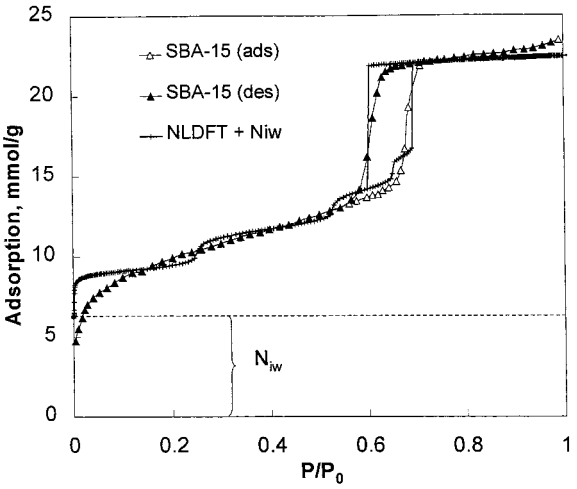

Figure 2. Comparison of the NLDFT adsorption isotherm in a 6.8 nm cylindrical pore with the isotherm on SBA-15 material[17] (sample S1-C in Table 1). The NLDFT isotherm is shifted by the amount adsorbed in intrawall pores, $N_{iw} = 6.2$ mmol/g. The surface area of the main mesopores is 315 m^2/g.

of intrawall pores. It is worth noting that the comparison plot method implies that the ranges of micropore and mesopore sizes do not overlap and the micropore filling is mostly completed prior to the region of polymolecular sorption and condensation in mesopores. It appears that in SBA-15 the range of intrawall porosity spans from the fractions to few nanometers. This means that sorption in the intrawall pores and growth of the adsorption film in the main channels cannot be properly separated, and therefore, the interval for regression cannot be chosen without ambiguity (see a typical plot in Figure 1 of ref 18).

Adsorption isotherms on SBA-15 materials exhibit a well-defined hysteresis loop of type H1 according to the IUPAC classification[27] (see Figure 2). This type of hysteresis loops is associated with capillary condensation and desorption in open-ended cylindrical mesopores. In such a structure, the conventional BJH method, which is based on the Kelvin equation for the hemispherical meniscus,[27] implies the use of the desorption branch of the isotherm for pore size calculations. However, in some cases,[1,3,20] the adsorption branch was used for the BJH calculations, which cannot be justified theoretically. Problematic as well is the fact that the BJH method does not take into account the influence of solid−fluid interactions on capillary condensation. As a consequence, the BJH method underestimates the pore size in the materials with pores as large as 20 nm.[28−31] This leads to overrated values (typically of 4−5 nm, see Figure 7 below) for the pore wall thickness.

Besides the BJH method, several other methods have been applied to the characterization of SBA-15 materials. Lukens et al.[4] and others[11−13] used a simplified Broekhoff−de Boer[32] method, in which the adsorption isotherm on nonporous surface is represented in the form of the FHH equation (so-called BdB−FHH method). Although the pore diameters calculated by the BdB−FHH method were shown to be in reasonable agreement with the transmission electron microscopy,[4] the amount of intrawall porosity has not been assessed. Kruk et al.[17] used an extrapolation of the empirical relation between the pore size and the capillary condensation pressure[33] obtained for MCM-41-like materials with pores smaller than the pores of the SBA-15 materials that they actually analyzed. As shown below, this approach leads to overrated (by ca. 1 nm) values of pore diameters.

In this work, we present a method for characterization of SBA-15 materials, which is based on the nonlocal density functional theory (NLDFT) of adsorption and capillary condensation hysteresis in cylindrical pores of siliceous materials.[29,34−36] The NLDFT method for pore size distribution (PSD) analysis was shown to provide reliable results for the MCM-41 type materials.[28,30,35] The validity of the NLDFT method was confirmed by (1) consistent PSD calculations from N_2 isotherms at 77 K, and Ar isotherms at 87 and 77 K,[28,31,35] (2) consistent PSDs in wide-pore materials calculated independently from the adsorption and desorption branches of the isotherms,[30,31,36] (3) quantitative agreement of the NLDFT results with the molecular simulations of the capillary condensation and hysteresis in cylindrical pores,[37] (4) smooth merging of the NLDFT results with the results of macroscopic thermodynamic methods in the limit of large pores,[31] and (5) good agreement of the pore diameters of MCM-41 type materials obtained by NLDFT method with the values obtained by independent methods.[38]

An important advantage of the NLDFT method as applied to SBA-15 materials is that, in addition to the mesopore size and the pore wall thickness, the method allows us to determine the volume of intrawall pores. In so doing, the pore structure parameters obtained by the NLDFT method are in agreement with a simple geometrical model of SBA-15. The NLDFT analysis removes some of the controversies in recent studies[21] of the pore structure of SBA-15 materials.

2. Nonlocal Density Functional Theory (NLDFT) Method

The NLDFT model allows one to calculate the adsorption−desorption isotherms in cylindrical pores. The NLDFT model for nitrogen and argon adsorption on siliceous materials was described in detail in our previous publications.[29,34,35] The parameters of the intermolecular potentials used in the model were chosen to provide good description of the bulk fluid equilibrium[35] and adsorption isotherms on nonporous silicas.[29,30]

It is worth noting that the pressures of capillary condensation and desorption in pores predicted by the NLDFT model are not very sensitive to variations of the parameters of solid−fluid interactions. For example, it has been shown that for a 6.9 nm cylindrical pore, which is at the lower limit of pore sizes in SBA-15 materials, even a 20% decrease or increase in the well depth of the solid−fluid potential shifts the predicted transition pressures by 0.015−0.02 P/Po.[39] In terms of pore diameters, this shift corresponds to variations within 0.2−0.3 nm, or 3−4%. Therefore, the NLDFT model with the parameters chosen to describe the adsorption isotherm on a nonporous substrate provides a robust and reliable method for pore size analysis from experimental isotherms.

Pore size distribution is determined from the deconvolution of the generalized adsorption equation, which represents the experimental isotherm as a weighted sum of the theoretical isotherms in pores of different diameters:

$$N_{exp}(P/P_0) = \int_{D_{min}}^{D_{max}} N_S(D,P/P_0)\varphi_S(D)\,dD \qquad (1)$$

Here, $N_S(D,P/P_0)$ is the theoretical isotherm in a pore of diameter D and $\varphi_S(D)$ is the pore size distribution function to be determined. The NLDFT method for the isotherms with H1 hysteresis loop uses two sets (kernels) of theoretical isotherms. The kernel of the theoretical equilibrium isotherms is used for calculations from the experimental desorption branches; the kernel of theoretical adsorption isotherms is used for calculations from the experimental adsorption branches. Foundations and limitations of this approach are discussed in refs 30, 31, and 38. For SBA-15 materials, which exhibit H1 hysteresis loops,

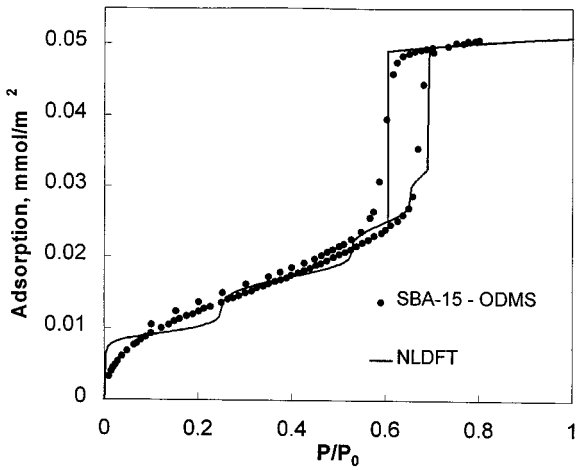

Figure 3. Comparison of the NLDFT adsorption isotherm in cylindrical pore of 6.7 nm in diameter with the isotherm on SBA-15 material modified with ODMS ligands (sample B from ref 18).

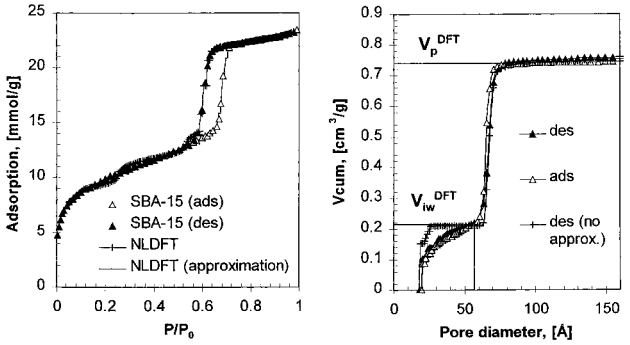

Figure 4. Left: nitrogen adsorption−desorption isotherms on SBA-15 material S1-C[17] (points) and fitted isotherms obtained by the NLDFT method without approximation (crosses) and with approximation for the multilayer adsorption (lines). Right: NLDFT cumulative pore volume distributions calculated from adsorption (open triangles) and desorption (closed triangles) branches. NLDFT pore volume distribution obtained from the desorption branch without approximation for the multilayer adsorption (crosses). V_p^{DFT} and V_{iw}^{DFT} are the total and intrawall pore volumes, respectively.

both branches of the experimental isotherm are, in principle, applicable for PSD calculations. Because the desorption branch of the experimental isotherm in cylindrical pores is more likely to correspond to the thermodynamic equilibrium,[34,37] it is preferable to employ the desorption branch, provided that it is not affected by networking effects. Note that the average pore size can be estimated from the inflection points of experimental adsorption and desorption isotherms using NLDFT pore size-pressure dependencies (see e.g. refs 30 and 31 for N_2 at 77 K and ref 31 for Ar at 87 K).

NLDFT calculations in cylindrical pores show that, because of confinement, the multilayer adsorption prior to the capillary condensation step is enhanced as compared to the adsorption on a nonporous surface. This effect has been incorporated in the present NLDFT method. One of the shortcomings of the NLDFT model is that the calculated isotherms exhibit pronounced layering at pressures below the capillary condensation transition[29] (see also examples in Figures 2 and 3 below). This layering is an artifact caused by the use of the simplified, structureless pore wall model and approximations made in the theory. Therefore, the multilayer adsorption isotherms in pores prior to the capillary condensation step were approximated as $N_S(D,P/P_0) = N_{STD}(P/P_0)(1 + \delta/D)$, where $N_{STD}(P/P_0)$ is the standard adsorption isotherm on nonporous silicas and $\delta = 0.9$ nm, thus taking into account the increase in adsorption due to confinement. This smoothening of the multilayer adsorption isotherms improves the fit to the experimental isotherm but, otherwise, has little influence on the pore size distributions obtained by the NLDFT method (see Figure 4 below). This approach was shown to be successful for the characterization of reference MCM-41[35] and several SBA-15[6] materials (see ref 38).

3. Results and Discussion

We have chosen from the literature several prominent examples of nitrogen adsorption isotherms on SBA-15 materials prepared with Pluronic P123 triblock copolymer ($EO_{20}PO_{70}EO_{20}$) in different research groups.[1,4,17,18,21] Other examples of characterization of micro−mesoporous and pure mesoporous SBA-15[6] are presented elsewhere.[38]

3.1. Evidence of the Existence of Intrawall Porosity from Adsorption Data. In our previous works, we showed that the NLDFT model quantitatively describes experimental adsorption isotherms on MCM-41 and related materials that do not contain microporosity (see, e.g., refs 30, 31, 37, and 38). We assume that this model is also adequate in order to account for adsorption in cylindrical mesopores of SBA-15 materials. Figure 2 shows the adsorption−desorption isotherm on one of the SBA-15 materials reported in ref 17. The isotherm has a typical hysteresis loop of type H1. This hysteresis loop is well approximated by the NLDFT isotherm in a cylindrical pore of 6.8 nm in diameter. However, the experimental isotherm exhibits a significant additional uptake prior to the capillary condensation step because of the adsorption in intrawall pores. Therefore, to fit the experimental isotherm, this contribution has to be added to the adsorption in cylindrical mesopores:

$$N^{theor}(P/P_0) = N_S^{DFT}(P/P_0)S_{meso} + V_{iw}\rho_L = N_S^{DFT}(P/P_0)S_{meso} + N_{iw} \quad (2)$$

where $N_S^{DFT}(P/P_0)$ is the NLDFT isotherm in the cylindrical mesopore per unit area, S_{meso} is the surface area of mesopores, V_{iw} is the volume of intrawall pores, and ρ_L is the normal liquid density of nitrogen. The theoretical isotherm computed in such a way is in agreement with the experimental one (Figure 2). The parameters are $V_{iw} = 0.22$ cm^3/g and $S_{meso} = 315$ m^2/g. This example is typical for adsorption isotherms on SBA-15, confirming that the intrawall porosity causes an additional contribution to the adsorption in main cylindrical mesopores.

Intrawall porosity can be reduced and even practically eliminated by chemical modification of SBA-15, as shown by Ryoo et al.,[18] with the example of chemical bonding of trimethylsilyl (TMS) and octyldimethylsilyl (ODMS) ligands. In the latter case, all intrawall porosity was effectively blocked by ODMS. The authors[18] estimated the range of intrawall pores between 1 and 3 nm. In Figure 3, we compare the NLDFT isotherm in a cylindrical pore of 6.7 nm with the isotherm on an ODMS-modified SBA-15.[18] It can be seen that the isotherm on modified SBA-15 is in good agreement with the theoretical isotherm in an ideal cylindrical pore. This result confirms that the modified sample does not contain intrawall pores. In these considerations, we neglect the difference between the adsorption isotherms on pure silicas and organically modified silicas, which is known to be important in the low-pressure region.[40,41] For ~7 nm cylindrical pores, the influence of the surface modification on the position of the capillary condensation and desorption steps is quite negligible, to within $0.02P/P_0$. These two examples

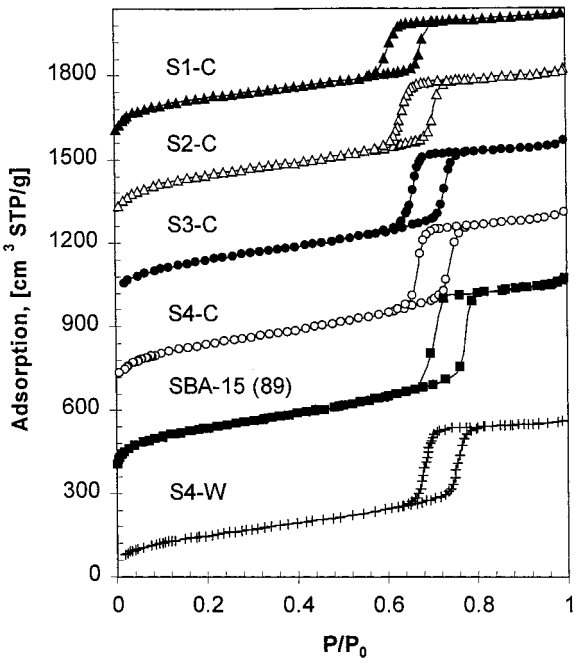

Figure 5. Nitrogen adsorption−desorption isotherms on SBA-15 materials[1,17] (see Table 1). Ordinates for samples SBA-15 (89) S4-C, S3-C, S2-C, and S1-C are shifted by 300, 600, 900, 1200, and 1500 cm^3(STP)/g, respectively.

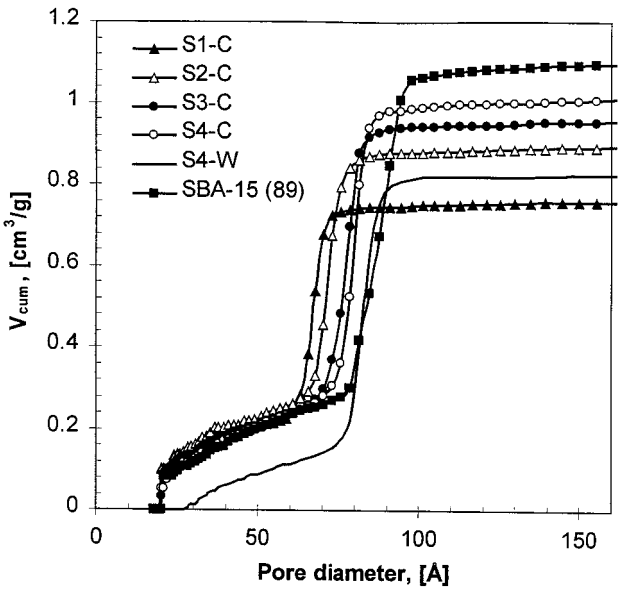

Figure 6. Cumulative pore volume distributions of SBA-15 materials[1,17] (see Table 1) calculated by the NLDFT method.

(Figures 2 and 3) show that the NLDFT method allows one to discriminate the intrawall porosity by comparing the experimental isotherms with the theoretical isotherms in cylindrical mesopores.

3.2. Calculation of Pore Size Distributions and Assessment of the Intrawall Porosity. By solving eq 1, we calculated the pore size distributions from the adsorption and desorption branches of the experimental isotherms using the kernels of theoretical NLDFT adsorption and equilibrium isotherms, respectively. The cumulative pore size distribution curves exhibit a prominent step, which corresponds to the main mesoporous channels of 6−7 nm in diameter, and a tail, which is attributed to the intrawall pores. Division between the two groups of pores is illustrated in Figure 4. This division is somewhat arbitrary; however, it leads to only minor variations in the estimated volume of intrawall pores, V_{iw}^{DFT}, and the volume of main mesopores, calculated as the difference between the total pore volume and the volume of intrawall pores, $V_p^{DFT} - V_{iw}^{DFT}$. The pore size distribution results obtained from the adsorption and desorption branches are in good agreement, confirming the reliability of the NLDFT model. Figure 4 also demonstrates that the use of the approximation for the multilayer adsorption isotherms improves the fit of the experimental isotherm in this region and does not change significantly the obtained pore size and other pore structure parameters.

In our calculations, the smallest pore size used in the NLDFT model was intentionally limited to 2 nm; we do not attempt to evaluate the actual distribution of micropores. It should be noted that the calculation of micropore distribution in SBA-15 from nitrogen adsorption isotherms is complicated because the low-pressure portions of the isotherms are typically smooth, thus indicating a broad distribution of micropores. Also, there is no underlying evidence to assume a specific shape of intrawall pores. This situation differs from the micropore analysis in other materials such as active carbons, where the molecular level methods of the density functional theory and Monte Carlo simulations in slit-shaped pores were shown to provide reasonable estimates for pore size distributions in the range 0.5−2 nm, see, e.g., recent works.[42−45]

Figure 5 presents a series of nitrogen isotherms on SBA-15 materials,[17] which were synthesized at 308 K, aged at different temperatures, washed with water or ethanol, and then calcined at 823 K to remove the polymeric template. For comparison, we also included the isotherm on uncalcined SBA-15, which was only washed with water[17] (sample S4-W), and the isotherm on calcined SBA-15 material, prepared from P123 copolymer under slightly different conditions as described by Zhao et al.[1] (sample SBA-15 (89)). We calculated the pore size distributions from the desorption branches. The cumulative pore volume distribution curves are presented in Figure 6. All of the samples possess a narrow distribution of the main channels in the range of 6−8 nm. The mean pore size and the total pore volume increase with higher aging temperature (from samples S1-C to S4-C), in agreement with the observations made in ref 17 (see Table 1). The specific volume of the intrawall pores is approximately the same for the calcined samples presented in Figure 5. The sample that was washed with water without subsequent calcination (sample S4-W) exhibits ca. half the amount of the intrawall porosity because of incomplete removal of the template. SBA-15 material reported by Zhao et al. has the largest unit cell size ($a_0 = 12.0$ nm) and the average NLDFT pore diameter of ca. 8.8 nm[1]. The NLDFT pore diameter is in agreement with the reported pore size of 8.9 nm[1].

3.3. Geometrical Model of SBA-15. A simple geometrical model supports the validity of the pore structure parameters obtained by the NLDFT method. In this model, we consider the main cylindrical channels arranged in a hexagonal array. The intrawall pores are assumed to be located within the silica matrix, and their detailed distribution is not important for the purpose of estimating the pore diameter of main channels. The pore diameter is calculated as

$$D_{cyl} = (\sqrt{(2\sqrt{3})/\pi})a_0\sqrt{\epsilon} \approx 1.05a_0\sqrt{\epsilon} \qquad (3)$$

where a_0 is the unit cell size, and

$$\epsilon = \rho_S(V_p^{DFT} - V_{iw}^{DFT})/(1 + \rho_S V_p^{DFT}) \qquad (4)$$

TABLE 1: Pore Structure Parameters of SBA-15 Materials Determined by Different Methods

sample	a_0[a] nm	ref	V_p^{DFT}[b] cm^3/g	V_{iw}^{DFT}[b] cm^3/g	D^{DFT}[c] nm	h^{DFT}[c] nm	D^{cyl}[d] nm	h^{cyl}[d] nm	V_{mi}^{cmp}[e] cm^3/g	D_e[f] nm	h_e[f] nm	D_{BJH}[g] nm	h_{BJH}[g] nm
S1-C	9.7	17	0.74	0.22	6.8	2.9	6.7	3.0	0.12	7.6	2.1	5.4	4.3
					6.6	*3.1*						*6.4*	*3.3*
S2-C	10.4	17	0.86	0.24	7.3	3.1	7.5	2.9	0.12	8.1	2.3	5.7	4.7
					7.0	*3.4*						*7.3*	*3.1*
S3-C	10.2	17	0.93	0.24	7.9	2.3	7.6	2.6	0.08	8.8	1.4	6.0	4.2
					7.6	*2.6*						*7.7*	*2.5*
S4-C	10.6	17	0.99	0.24	8.1	2.5	8.0	2.6	0.06	9.0	1.6	6.4	4.2
					7.7	*2.9*						*8.1*	*2.5*
S4-W	11.2	17	0.82	0.12	8.5	2.7	8.7	2.5	n/a	9.5	1.7	6.8	4.4
					8.2	*3.1*						*8.1*	*3.1*
SBA-15	11.6	4	1.15	0.34	8.8	2.8	8.7	2.9	n/a	n/a	n/a	7.2	4.4
					8.5	*3.1*						*9.0*	*2.6*
SBA-15 (89)	12.0	1	1.08	0.28	8.8	3.2	9.1	2.9	n/a	n/a	n/a	7.3	4.7
					8.6	*3.4*						*9.0*	*3.0*

[a] a_0 is the XRD unit cell parameter. [b] V_p^{DFT} and V_{iw}^{DFT} are respectively the total pore volume and the volume of intrawall pores determined by the NLDFT method. [c] D^{DFT} and h^{DFT} are the pore diameter and the minimal pore wall thickness determined by the NLDFT method from the desorption branch (upper row) and from the adsorption branch (lower row, in italic). [d] D^{cyl} and h^{cyl} are the pore diameter and the wall thickness calculated from the geometrical model (eq 3) using V_p^{DFT} and V_{iw}^{DFT}. [e] V_{mi}^{cmp} is the micropore volume determined in ref 17 from the comparison plot method. [f] D_e and h_e are the pore diameter and the wall thickness obtained in ref 17 by the empirical method. [g] D_{BJH} and h_{BJH} are the pore diameter and the wall thickness calculated by the BJH method[27] using the equation for the hemispherical meniscus applied to the desorption (upper row) and adsorption (lower row, in italic) branches.

is the volume fraction of the main channels (mesoporosity); V_p^{DFT} and V_{iw}^{DFT} are the total pore volume of micro- and mesopores and the volume of intrawall pores, respectively; ρ_S is the skeleton density of silica matrix, which we assume to be equal to the density of amorphous silica (2.2 g/cm^3). Alternatively, one could use the volume of the main channels and an apparent density of silica walls with intrawall pores included. However, this density is unknown. The present approach avoids this difficulty by using the volume of intrawall pores evaluated from adsorption data. Comparison of the pore diameters calculated by the NLDFT method with those estimated from the geometrical considerations is shown in Table 1. The agreement is quite convincing, to within 0.3 nm for most samples.

3.4. Comparison of Different Methods of Interpretation of Adsorption Data on SBA-15. In Table 1, we compare the pore structure parameters obtained by different methods. The BJH method, when applied to the desorption branch of the isotherm, underestimates the pore diameter by ca. 20−25%. When the adsorption branch is taken for the BJH calculations, which is theoretically incorrect, the results seem to agree with the NLDFT method. This agreement is, however, purely accidental and should not be regarded as a confirmation of the BJH method validity. The reasons for the inaccuracy of the BJH method were discussed in details in previous publications.[28,29,31] The pore diameters of SBA-15 materials estimated by the method of Kruk et al.[17] are ca. 0.8−0.1 nm larger than those calculated by the NLDFT method (Table 1).

Table 1 also shows that the micropore volumes obtained in ref 17 using the comparison plot method are significantly lower (up to 4 times) than the total volumes of intrawall pores evaluated from the NLDFT method. Presumably, this difference is due to the fact that the overlapping regions of sorption in intrawall micropores, narrow mesopores, and polymolecular adsorption on the surface of the main channels cannot be properly separated using the comparison plot method.

According to the NLDFT method, the intrawall pores occupy ca. 20−40% of the pore wall. The minimal pore wall thickness was calculated as the difference between the unit cell size a_0 and the pore diameter. The pore wall thicknesses calculated using pore diameters obtained by different methods are shown

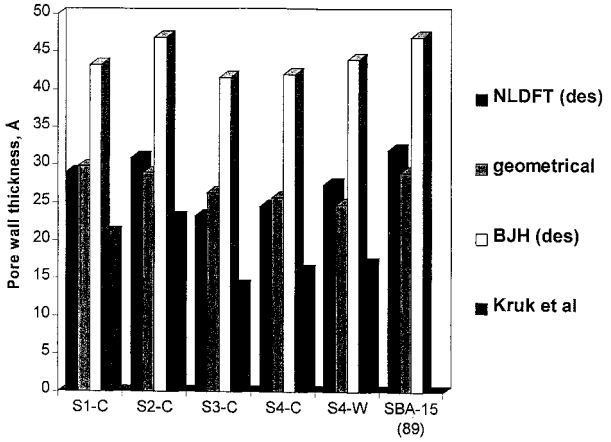

Figure 7. Minimal pore wall thickness of SBA-15 materials[1,17] determined by different methods (see Table 1).

in Table 1 and in Figure 7. For these samples, the wall thickness is in the range of 2.5−3.4 nm. It is seen that, although the unit cell size, the pore volume, and the mesopore size increase with the aging temperature, the pore wall thickness and the volume of intrawall pores remain practically unchanged. As compared to the NLDFT method, the BJH method overestimates the pore wall thickness by ca. 50−80%, whereas the method of Kruk et al.[17] underestimates it by ca. 30−40%.

Figures 8 and 9 illustrate the evolution of the pore structure parameters of SBA-15 materials during the preparations described in the paper of Ryoo et al.[18] (see Table 2). The sample was washed in water to partially remove the template, and then the material was subjected to thermal treatment at elevated temperatures of up to 1273 K. The initial water-washed sample (sample S4-W from Table 1) has the pore size of ca. 8.5 nm, the total pore volume of 0.82 cm^3/g, and the volume of intrawall pores of 0.12 cm^3/g. Calcination at 823 K removes the polymeric template from the wall; the calcined material has the pore size of 8.0 nm, the total pore volume of 0.98 cm^3/g, and a significant volume of intrawall pores (0.27 cm^3/g). Subsequent heating at higher temperatures leads to condensation of the silica framework and gradual elimination of the intrawall porosity. The materials heated to 1073 and 1173 K exhibit smaller pore sizes and volumes of micro- and mesopores. The material heated to

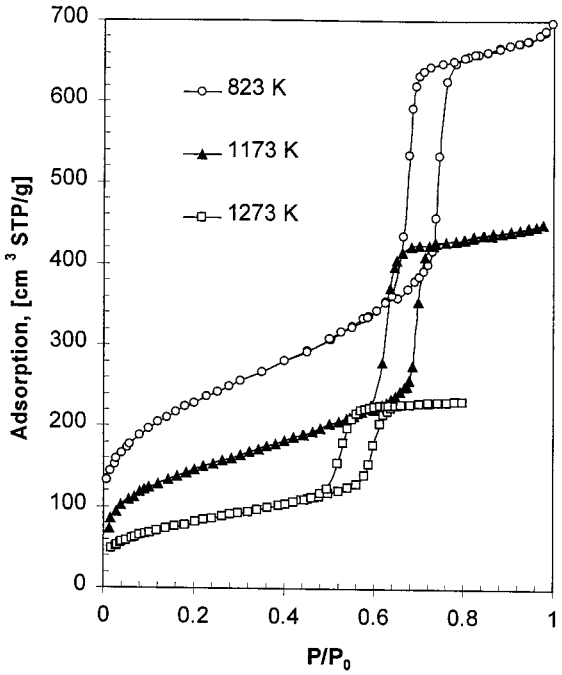

Figure 8. Nitrogen adsorption−desorption isotherms on SBA-15 materials[18] calcined at 823 K and subsequently heated at temperatures up to 1273 K (see Table 2).

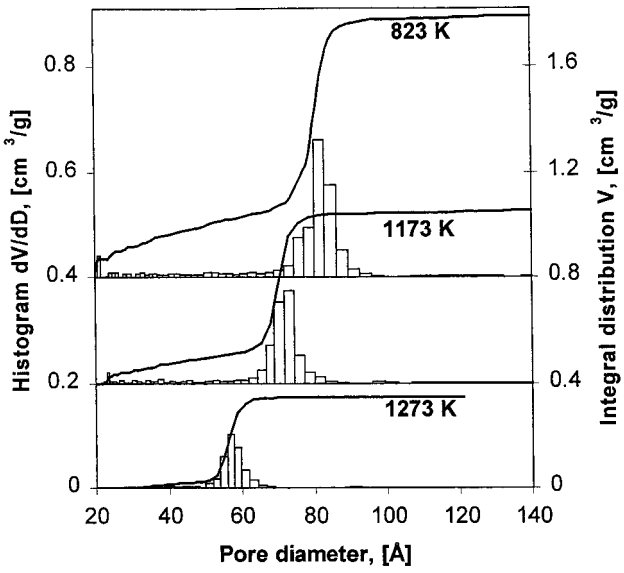

Figure 9. NLDFT pore size distributions of SBA-15 materials[18] calcined at 823 K and subsequently heated at temperatures up to 1273 K (see Table 2).

TABLE 2: Pore Structure Parameters of the SBA-15 Material Calcined at Elevated Temperatures[18] as Determined by the NLDFT Method

sample	V_p^{DFT} cm^3/g	V_{iw}^{DFT} cm^3/g	D^{DFT} nm	S_p^{DFT} m^2/g	D^{DFT} S_p^{DFT}/V_p^{DFT}	V_p^{DFT}/S_p^{DFT} nm
washed	0.82	0.12	8.5	460	4.8	1.8
823	0.98	0.27	8.0	690	5.6	1.4
973	0.84	0.20	7.8	600	5.6	1.4
1073	0.74	0.16	7.4	516	5.2	1.4
1173	0.64	0.12	7.0	440	4.8	1.5
1273	0.35	0	5.7	250	4.1	1.4

1273 K has a regular structure, with no intrawall porosity/roughness, and with the pore volume almost three times smaller than that of the original material calcined at 823 K (see Figure 9 and Table 2).

It is interesting to note that for the samples listed in Table 2 the adsorption isotherms normalized by the amount adsorbed after the pore filling (at $P/P_0 = 0.8$) become practically identical in the multilayer adsorption region (this follows from Figure 9 in ref 18). Thus, the ratio of the total pore volume to the total surface area is the same for all of these samples. The pore structure parameters obtained by the NLDFT method fully support this peculiar observation. The ratio $V_p^{DFT}/S_p^{DFT} \approx 1.4$ nm is characteristic of all calcined samples listed in Table 2. Note that for samples treated at elevated temperatures the ratio $(D^{DFT}S_p^{DFT})/V_p^{DFT}$ (wS/V parameter) decreases as the intrawall porosity decreases, in agreement with the conclusions of Ryoo et al.[18] However, the wS/V values presented in ref 18 are larger than the NLDFT values by ca. 20%. The wS/V ratios calculated by the NLDFT method are more accurate, and for the sample with no intrawall microporosity (heated at 1273 K), the NLDFT method gives $(D^{DFT}V_p^{DFT})/S_p^{DFT} = 4.1$, in good agreement with what can be expected for cylindrical pores (see Table 2).

3.5. Comparison with X-ray Diffraction Data. We have compared the pore diameters of SBA-15 obtained by the NLDFT method with the results of modeling X-ray diffraction intensities reported by Imperor-Clerc et al.[21] The authors considered four structural models of SBA-15: (1) a one parameter model based on two density levels (pore and silica), (2) a two parameter model with two density levels and a fluctuating position of cylindrical pores, (3) a three parameter model with three density levels (pore, corona of uniform low density silica, and dense silica), and (4) a two parameter model with the corona of linearly increasing density. The first model was discarded because it did not describe the experimental X-ray diffraction intensities properly. In our opinion, the results obtained with the other three models were comparable (the best fit was obtained with the model 3 which has one additional parameter). However, the authors[21] discarded model 2 because it predicted much larger pore diameters than the values obtained from nitrogen adsorption isotherms using the BJH method. Thus, it was concluded that only the models involving a corona of low-density silica (models 3 and 4) can adequately describe the structure of SBA-15 materials. Without arguing the validity of different structural models, we give below our analysis of the adsorption isotherm data published in ref 21.

The capillary condensation of nitrogen in SBA-15 sample P123 BC occurs at the relative pressure of ca. $P/P_0 = 0.77$, and the desorption occurs at ca. $P/P0 = 0.69$ (see Figure 3 in ref 21). According to the NLDFT model, this corresponds to the pore diameter of 8.5 nm and the pore radius/unit cell ratio of 0.385. These values are in good agreement with the pore diameter of 8.2 nm and the ratio of 0.372 obtained from X-ray diffraction using the two-density model with a 10% fluctuating position of the cylindrical channels (see Table 4 in ref 21). As compared with other models, the NLDFT pore diameter of 8.5 nm falls between the corona diameter of 7 nm and the dense silica core diameter of 9.4 nm determined from the uniform corona model.[21] The same applies to the model of increasing corona density, which spans from 5.8 to 10.4 nm. We calculated the pore size distribution by the NLDFT method and obtained the total pore volume of 1.0 cm^3/g and the volume of intrawall pores of ca. 0.15 cm^3/g. These values correspond to the "geometrical" pore size (Equation 3) of ca. 8.9 nm, which is in good agreement with the NLDFT pore diameter of 8.5 nm and in no contradiction with the data obtained from X-ray intensities. For the second sample reported in ref 21 designated as P123 AC, the capillary condensation occurs at ca. $P/P_0 = 0.62$. The NLDFT model predicts the pore size of ca. 5.8 nm, to be

compared to the corona diameter of 5 nm and the silica diameter of 7 nm according to the three-density level model. Unfortunately, the authors did not indicate the pore diameter of this sample obtained from the two-density model with the fluctuating channel position.

From this example, we conclude that the pore diameters of SBA-15 obtained by the NLDFT method are in reasonable agreement with the values obtained from modeling the X-ray data,[21] even without invoking the models involving the corona of low-density silica. The apparent discrepancy between the mesopore diameters obtained from X-ray and adsorption data was caused by the use of the BJH method, which underestimates the pore size.

4. Conclusions

We developed a consistent method for evaluating the pore structure parameters of SBA-15 materials from adsorption and desorption isotherms based on the NLDFT model of capillary condensation and hysteresis in open cylindrical pores. The NLDFT method permits independent determination of pore size distributions from the adsorption and desorption branches of experimental isotherms using two different sets of theoretical isotherms, for adsorption and desorption calculations, respectively.

SBA-15 materials templated by triblock copolymers contain an appreciable amount of intrawall pores, up to 30% of the total porosity. The NLDFT method allows one to calculate the size distribution of the main mesoporous channels and the total volume of the intrawall pores. The structural parameters obtained by the NLDFT method are in good agreement with simple geometrical considerations. At the same time, appreciable deviations are found between the NLDFT method and other pore size analysis methods used in the literature. Indeed, for typical SBA-15 materials with mesopore diameters of ca. 6.5−9 nm according to the NLDFT method, the standard BJH method, when applied to the desorption branch of the isotherm, gives ca. 20−25% smaller pore diameters and ca. 50−80% larger minimal pore wall thickness. The empirical method used in ref 17 gives ca. 10−12% larger pore size than the NLDFT method. It is also shown that the micropore volumes determined using the comparison plots are significantly lower than the total volumes of intrawall pores obtained by the NLDFT method. The analysis of adsorption isotherms on SBA-15 by the NLDFT method resolves some of the recently published discrepancies between the pore sizes determined by different methods. Particularly, it is shown that the pore diameters of SBA-15 materials obtained by the NLDFT method are in accord with the pore diameters obtained in quantitative modeling of X-ray diffraction patterns.[21] The NLDFT method is recommended for the characterization of SBA-15 and related micro−mesoporous materials.

Acknowledgment. This work has been supported in part by the TRI/Princeton exploratory research program and EPA Grant R825959-010.

References and Notes

(1) Zhao, D. Y.; Feng, J. L.; Huo, Q. S.; Melosh, N.; Fredrickson, G. H.; Chmelka, B. F.; Stucky, G. D. *Science* **1998**, *279*, 548.
(2) Zhao, D. Y.; Huo, Q. S.; Feng, J. L.; Chmelka, B. F.; Stucky, G. D. *J. Am. Chem. Soc*. **1998**, *120*, 6024.
(3) Zhao, D. Y.; Yang, P. D.; Melosh, N. A.; Feng, J. L.; Chmelka, B. F.; Stucky, G. D. *Adv. Mater.* **1998**, *10*, 1380.
(4) Lukens, W. W.; Schmidt-Winkel, P.; Zhao, D. Y.; Feng, J. L.; Stucky, G. D. *Langmuir* **1999**, *15*, 5403.
(5) Yue, Y. H.; Gedeon, A.; Bonardet, J. L.; Melosh, N.; D'Espinose, J. B.; Fraissard, J. *Chem. Commun*. **1999**, 1967.
(6) Yue, Y. H.; Gedeon, A.; Bonardet, J. L.; D'Espinose, J. B.; Melosh, N.; Fraissard, J. *Stud. Surf. Sci. Catal.* **2000**, *129*, 209.
(7) Luan, Z. H.; Maes, E. M.; van der Heide, P. A. W.; Zhao, D. Y.; Czernuszewicz, R. S.; Kevan, L. *Chem. Mater*. **1999**, *11*, 3680.
(8) Luan, Z. H.; Hartmann, M.; Zhao, D. Y.; Zhou, W. Z.; Kevan, L. *Chem. Mater*. **1999**, *11*, 1621.
(9) Han, Y. J.; Stucky, G. D.; Butler, A. *J. Am. Chem. Soc*. **1999**, *121*, 9897.
(10) Luan, Z. H.; Bae, J. Y.; Kevan, L. *Chem. Mater*. **2000**, *12*, 3202.
(11) Feng, P. Y.; Bu, X. H.; Stucky, G. D.; Pine, D. J. *J. Am. Chem. Soc*. **2000**, *122*, 994.
(12) Feng, P. Y.; Bu, X. H.; Pine, D. J. *Langmuir* **2000**, *16*, 5304.
(13) Morey, M. S.; O'Brien, S.; Schwarz, S.; Stucky, G. D. *Chem. Mater*. **2000**, *12*, 898.
(14) Margolese, D.; Melero, J. A.; Christiansen, S. C.; Chmelka, B. F.; Stucky, G. D. *Chem. Mater*. **2000**, *12*, 2448.
(15) Lettow, J. S.; Han, Y. J.; Schmidt-Winkel, P.; Yang, P. D.; Zhao, D. Y.; Stucky, G. D.; Ying, J. Y. *Langmuir* **2000**, *16*, 8291.
(16) Liu, A. M.; Hidajat, K.; Kawi, S.; Zhao, D. Y. *Chem. Commun*. **2000**, 1145.
(17) Kruk, M.; Jaroniec, M.; Ko, C. H.; Ryoo, R. *Chem. Mater*. **2000**, *12*, 1961.
(18) Ryoo, R.; Ko, C. H.; Kruk, M.; Antochshuk, V.; Jaroniec, M. *J. Phys. Chem. B* **2000**, *104*, 11465.
(19) Jun, S.; Joo, S. H.; Ryoo, R.; Kruk, M.; Jaroniec, M.; Liu, Z.; Ohsuna, T.; Terasaki, O. *J. Am. Chem. Soc*. **2000**, *122*, 10712.
(20) Miyazawa, K.; Inagaki, S. *Chem. Commun*. **2000**, 2121.
(21) Imperor-Clerc, M.; Davidson, P.; Davidson, A. *J. Am. Chem. Soc*. **2000**, *122*, 11925.
(22) Jang, J. S.; Lim, B.; Lee, J.; Hyeon, T. *Chem. Commun*. **2001**, 83.
(23) Newalkar, B. L.; Olanrewaju, J.; Komarneni, S. *Chem. Mater*. **2001**, *13*, 552.
(24) Beck, J. S.; Vartuli, J. C.; Roth, W. J.; Leonowicz, M. E.; Kresge, C. T.; Schmitt, K. D.; Chu, C. T. W.; Olson, D. H.; Sheppard, E. W.; McCullen, S. B.; Higgins, J. B.; Schlenker, J. L. *J. Am. Chem. Soc*. **1992**, *114*, 10834.
(25) De Paul, S. M.; Zwanziger, J. W.; Ulrich, R.; Wiesner, U.; Spiess, H. W. *J. Am. Chem. Soc*. **1999**, *121*, 5727.
(26) Melosh, N. A.; Lipic, P.; Bates, F. S.; Wudl, F.; Stucky, G. D.; Fredrickson, G. H.; Chmelka, B. F. *Macromolecules* **1999**, *32*, 4332.
(27) Gregg, S. J.; Sing, K. S. W. *Adsorption, Surface Area and Porosity*; Academic Press: New York, 1982.
(28) Ravikovitch, P. I.; Wei, D.; Chueh, W. T.; Haller, G. L.; Neimark, A. V. *J. Phys. Chem. B* **1997**, *101*, 3671.
(29) Ravikovitch, P. I.; Haller, G. L.; Neimark, A. V. *Adv. Colloid Interface Sci*. **1998**, *77*, 203.
(30) Ravikovitch, P. I.; Neimark, A. V. *Stud. Surf. Sci. Catal.* **2000**, *129*, 597.
(31) Neimark, A. V.; Ravikovitch, P. I. *Microporous Mesoporous Mater.* **2001**, *44-45*, 697.
(32) Broekhoff, J. C.; de Boer, J. H. *J. Catal*. **1968**, *10*, 368.
(33) Jaroniec, M.; Kruk, M.; Sayari, A. *Stud. Surf. Sci. Catal.* **2000**, *129*, 587.
(34) Ravikovitch, P. I.; O'Domhnaill, S. C.; Neimark, A. V.; Schuth, F.; Unger, K. K. *Langmuir* **1995**, *11*, 4765.
(35) Neimark, A. V.; Ravikovitch, P. I.; Grun, M.; Schuth, F.; Unger, K. K. *J. Colloid Interface Sci*. **1998**, *207*, 159.
(36) Neimark, A. V.; Ravikovitch, P. I. *Stud. Surf. Sci. Catal.* **2000**, *128*, 51.
(37) Neimark, A. V.; Ravikovitch, P. I.; Vishnyakov, A. *Phys. Rev. E* **2000**, *62*, R1493.
(38) Ravikovitch, P. I.; Neimark, A. V. *Colloids Surf. A* **2001**, *11*, 187−188.
(39) Ravikovitch, P. I.; Haller, G. L.; Neimark, A. V. *Stud. Surf. Sci. Catal.* **1998**, *117*, 77.
(40) Gobet, J.; sz. Kovats, E. *Ads. Sci. Technol*. **1984**, *1*, 285.
(41) Kruk, M.; Antochshuk, V.; Jaroniec, M.; Sayari, A. *J. Phys. Chem. B* **1999**, *103*, 10670.
(42) Ravikovitch, P. I.; Vishnyakov, A.; Russo, R.; Neimark, A. V. *Langmuir* **2000**, *16*, 2311.
(43) Dombrowski, R. J.; Hyduke, D. R.; Lastoskie, C. M. *Langmuir* **2000**, *16*, 5041.
(44) El-Merraoui, M.; Aoshima, M.; Kaneko, K. *Langmuir* **2000**, *16*, 4300.
(45) Sweatman, M. B.; Quirke, N. *J. Phys. Chem. B* **2001**, *105*, 1403.